



LJMU Research Online

Opoz, TT, Yasar, H, Ekmekci, N and Ekmekci, B

Particle Migration and Surface Modification on Ti6Al4V in SiC Powder Mixed Electrical Discharge Machining

<http://researchonline.ljmu.ac.uk/7772/>

Article

Citation (please note it is advisable to refer to the publisher's version if you intend to cite from this work)

Opoz, TT, Yasar, H, Ekmekci, N and Ekmekci, B (2018) Particle Migration and Surface Modification on Ti6Al4V in SiC Powder Mixed Electrical Discharge Machining. Journal of Manufacturing Processes, 31. pp. 744-758. ISSN 1526-6125

LJMU has developed **LJMU Research Online** for users to access the research output of the University more effectively. Copyright © and Moral Rights for the papers on this site are retained by the individual authors and/or other copyright owners. Users may download and/or print one copy of any article(s) in LJMU Research Online to facilitate their private study or for non-commercial research. You may not engage in further distribution of the material or use it for any profit-making activities or any commercial gain.

The version presented here may differ from the published version or from the version of the record. Please see the repository URL above for details on accessing the published version and note that access may require a subscription.

For more information please contact researchonline@ljmu.ac.uk

<http://researchonline.ljmu.ac.uk/>

Particle Migration and Surface Modification on Ti6Al4V in SiC Powder Mixed Electrical Discharge Machining

Tahsin T. Öpöz ^{a,*}, Hamidullah Yaşar^b, Nihal Ekmekci^b, Bülent Ekmekci^b

^aGeneral Engineering Research Institute, Liverpool John Moores University, Liverpool, L3 3AF, UK

^bMechanical Engineering Department, Bülent Ecevit University, Incivez 67100, Zonduldak, Turkey

*Corresponding author: E-mail: t.t.opoz@ljmu.ac.uk

Abstract

The study examines the impact of SiC powder concentration on surface topography, particles deposition and subsurface structures in powder mixed electrical discharge machining (PMEDM) of Ti-6Al-4V-ELI work material. It was observed that low pulse currents and high suspended particle concentration in dielectric liquid enhance the material transfer mechanism in particulate form. The subsurface properties of such surfaces exhibited a distinctive and harder re-solidified layer structure that indicates a unique material transfer mechanism takes place during machining. The particles placed close to a discharge column directed towards the melted metal pool due to the sudden closure of the plasma channel. When the main discharge channel subdivided into several secondary discharges, the suspended particles in dielectric liquid stuck among the scattered sub discharges and increased the probability of penetrating into the melted metal pool at the end of a discharge. Therefore, the formation of secondary discharges favoured the improved SiC transfer in particulate form. However, increasing the pulse current deplete the material transfer mechanism in particulate form due to the inadequacy of secondary discharges.

Keywords: Powder Mixed Electrical Discharge Machining; Ti-6Al-4V; particle migration

1. Introduction

Titanium and its alloys have been widely used in various industries such as aerospace and biomedical, due to their unique materials properties such as the high strength-to-weight-ratios,

excellent corrosion resistance, and biocompatibility [1, 2]. Electrical discharge machining (EDM) is a non-conventional machining process and highly effective for hard to cut materials such as titanium and its alloys. Desired surface characteristics of the materials and material removal can be controlled by choosing appropriate operational parameters of EDM. The material removal mechanism, dissimilar to the conventional machining methods, is based on the thermal effects of sequentially applied electrical sparks between electrodes (the work material and the tool) immersed in dielectric liquid. Therefore, the resultant surface quality and machining performance mainly rely on the thermal properties of the materials evolved in the process. When an electrical spark is generated in the inter-electrode gap, the temperatures and pressure increase rapidly to extreme values at incident regions. Therefore, a small fraction of the electrode materials is super-heated during sparking period. When the spark ceases, the super-heated material blows into the dielectric liquid and instantaneously solidified in the form of the sphere like features (debris). Similarly, the swept region of the electrode surfaces also cools down in extreme rates and leaves a tiny crater behind. The flow of the dielectric liquid takes away the debris particles and cleans the inter-electrode gap for the next sparking cycle.

The addition of fine powder in the dielectric liquid, named as powder mixed electrical discharge machining (PMEDM), can enhance the machining performance regarding material removal rate (MRR), tool wear rate (TWR), and modification of surface and subsurface characteristics. In this study, the effect of SiC powder concentration in the dielectric liquid in PMEDM of the titanium alloy (Ti-6Al-4V-ELI) is investigated to explore the change in surface topography widely, and distinct heat affected sublayers.

In the earliest study, better surface roughness was observed due to added impurities into the dielectric liquid [3]. Similarly, MRR increased 60%, and TWR decreased 28% with the addition of fine graphite powder into kerosene [4] and similar results found in [5, 6].

Kuriachen and Mathew [7] investigated the effect of the SiC powder concentration (5, 15 and 25 g/l) on MRR and TWR in micro electrical discharge machining of Ti-6Al-4V, the results showed the powder concentration of 5 g/l give higher MRR and lower TWR. The powder particles get polarised and form chains between the tool electrode and the workpiece [8]. Thus, decrease the insulation resistance of dielectric liquid and ease the formation of the electrical discharges. The presence of silicon powders in dielectric fluid also reduced the number of unwanted types of discharges such as arcs and short circuits [9]. Rehbein et al. [10] argued that a simple cylindrical electrical discharge model is inadequate in explaining the

crater shapes obtained and concluded that primary discharge channel breaks up in different forms during PMEDM. Ekmekci and Ersöz [11] highlighted that the role of powders in the dielectric liquid is not only about reducing the electrical field intensity and the insulating resistance of dielectric but also the particles placed around the plasma channel that alloyed the machined surface. Amorim et al. [12] investigated the molybdenum powder mixing with different size of powder particles on AISI H13 tool steel and detected Fe-Mo, MoC, and Mo crystalline phases in the modified layers.

Most of the researchers studied the PMEDM using SiC powders in the dielectric liquid to study the performance of EDM regarding material and tool wear rates. SiC particle migration to the machined surface usually mentioned as observed cases under specific machining conditions. The description of the mechanism, as well as the possible consequences on the heat damage layers, could not be well described in the literature. The current study elaborates the mentioned specific conditions with a plausible explanation of discharging mechanism and corresponding operational conditions which yield particle penetration on the surface.

Alterations on the and beneath the surface were examined to explore the possible impact of SiC migration.

The material migration mechanism from the dielectric liquid was discussed for the case of hydroxyapatite powder mixing in EDM [13], and the optimal machining parameters for hydroxyapatite deposition on the Ti-6Al-4V surfaces were suggested. Li et al. [14] studied Ti-6Al-4V Ti alloy with Cu-SiC composite tool electrode and demonstrated that TiC and TiSi₂ phases formed on the surface. Shabgard and Khosrozadeh [15] added carbon nanotubes in the dielectric when machining Ti-6Al-4V alloy work material and indicated a decrease in the surface roughness. SiC powder mixing using Ti-6Al-4V work material was also studied by Li et al. [16]. They pointed out the increase in microhardness due to the formation of TiC and TiSi₂ phases on the surface. In a recent study, the increase in the surface quality of Ti-35Nb-7Ta-5Zr, β -phase titanium alloy is also pointed out in the case of silicon powder mixing [17].

SiC powder addition in water dielectric liquid revealed various types of topographical features on Ti-6Al-4V surfaces suggesting machining is accompanied by subdivided electrical discharges in different forms [18,19]. Moreover, the material migration phenomenon from the dielectric liquid and the built up to the machined surface was also closely related to the forms of discharges. The suspended particles those are close to a discharge channel heated and then accelerated through the molten material when the electrical pulse ceases. The knowledge on

discharge separation and its interactions with the suspended particles is limited and needs further elaboration.

It is well-known that silicon carbide (SiC) is a very hard material commonly used in industry where hardness is required. Maximum hardness values from the subsurface layers are expected by using the SiC powder as an additive. However, the broad ranges of parameters such as in pulse time and pulse current affect the surface properties and the outcomes of the machining. Powder additive has a significant role in the formation of well-balanced discharge conditions results in improved surface and subsurface properties. Therefore, the study focused on the effect of the powder concentration on surface roughness, the numbers of deposited SiC particles and microhardness variation in PMEDMed Ti-6Al-4V work material.

2. Materials and Methods

In this study, a α - β titanium alloy, Ti-6Al-4V Extra Low Interstitial (ELI), is examined (Table 1). Ti-6Al-4V ELI workpiece material was provided by G&S Titanium, Inc. USA. The samples of 10 mm in diameter were cut ~8 mm height and turned. In an attempt to provide the parallelism between the workpiece and the tool electrode, all the samples and tool electrode were polished to ground before machining.

Samples were machined using AJAN EDM CNC 983 die sinking-type EDM. The dielectric liquid circulation system of the machine was disconnected, and a plastic liquid container was installed on the machine table with proper fixtures to handle the samples. A schematic view of the machine setup and a photo from the reservoir is shown in Figs. 1(a) and (b), respectively. 18 samples were electrical discharge machined using parametrical ordering in deionized water mixed with green 800 mesh SiC fine powders. Taguchi L18 orthogonal array was used to designate the EDM parameters to understand the possible impacts on the particles' deposition to the surface. Three parameters were selected as factors (Pulse current, pulse on time and SiC powder concentration) and mixed levels were used as 2, 3, 3, respectively (Table 2). The input parameters and results are shown in Table 3. Aluminum 6081 T6 was the tool material with positive polarity. The dielectric liquid was continuously stirred with a mechanical mixer to avoid suspended powder precipitation and accumulation.

The topographical and compositional analyses of the machined surfaces were examined using EDS equipped Quanta 450 Field Emission Gun (FEG) Scanning Electron Microscopy. The structure of the resolidified layers was identified using PANalytical EMPYREAN X-ray diffractometer equipped with Cu target and graphite single crystal monochromator. The

working conditions were 40 KV and 40 mA for both analyses. Data were collected using Cu-K α radiation ($\lambda=1.5405 \text{ \AA}$) between 20° and 90° in 2θ . The phases were identified from searches in the JCPDS (Joint Committee on Powder Diffraction Standards) database. 3D images of the surfaces were taken with Bruker 3D Contour GT-K 3D optical microscope equipped with Vision 64 software. The number of SiC particles deposited to the EDMed surfaces was counted from one clear, high-resolution SEM image with an area of 0.1133 mm^2 of each sample (Fig. 2). Then, predicted numbers of the particle expanded to the unit area in mm^2 . Only sharp-edged particles accepted as SiC particles migrated from the dielectric to the surface.

Machined samples were cross-sectioned to examine microstructural subsurface properties. All cross-sectioned samples were moulded and prepared with standard metallographic procedures as shown in Fig. 1(c). The samples were etched using Weck's reagent (100 ml pure water, 5 g Ammonium bifluoride) and immersed for 20 seconds to reveal the microstructural layers in the heat affected layers. Metkon IMM 901 optical microscope equipped with Clemex Captiva image analysing software was used to analyse the cross-sectioned samples.

The average Vickers microhardness values were measured with Shimadzu HMV-G21 (Vickers) micro-hardness tester based on five successful indentations using 98.087 mN indentation loads for 25 seconds. Microhardness was measured from the sections. An image of indentation during micro hardness measurement is presented in Fig. 3. The thicknesses of layers were measured from the section via Image-J software and based on the average of twenty equidistant measurements, which was taken from two adjacent views from the same section; each comprises ten measurements. The hardest layer is called dark layer which is on the top of all. In some cases of the sectional analyses, dendritic features (i.e. dendritic layer) which represent the confrontation of phase change isotherms are observed beneath the dark layer. The white layer is a fine structure of α phase rich region where phase transformation occurred in the liquid phase. After this thin white layer, a tempered zone and lastly the base structure of the work material are followed as shown in Fig. 1(d).

3. Results and discussion

3.1 Surface topography and roughness

Application of successive discharges produced overlapped craters over the surface of the machined parts. Crater rims and spherical like structures attached to it are the characteristic

signs of molten material flow and boiling during discharging. Such features are frozen abruptly at the end of discharge due to the high heat transfer rates attained due to convection from the dielectric liquid and conduction from the base material. However, the addition of SiC powders into dielectric liquid and using specific electrical parameters alter the breakdown conditions during discharging and result in different surface topographical features which could not be described with single column discharges. The main channel sprayed into secondary sub-discharges in various forms such as the case when the pulse on time is 100 μ s and pulse current is 2 A in 5 g/l SiC powder mixed dielectric liquid in Fig. 4(a). Larger craters formed due to the primary discharges and the pebbling-like features built due to the secondary ones. The main discharge channel activity gradually suppressed with an increase in powder concentration to 10 g/l as shown in Fig. 4(b). Finally, the channel activity disappeared, and the surface covered with small craters with further increase in concentration to 20 g/l in Fig. 4(c). Moreover, close examination of the surface by using backscattering and energy dispersive spectroscopy (EDS) revealed deposition of powder particles from the dielectric liquid during machining as shown in Fig. 5. Sharp-edged particles that are different from the traditional surface features are detectable as shown in Fig. 5(a). EDS analyses of the whole area in Fig. 5(b) and selected pointal region on a particle Fig. 5(c) revealed Si peaks which can only be transferred from SiC powder mixed dielectric liquid. The carbon peak has a low intensity since it was taken from the whole surface. It is accepted as typical by the authors because the samples were machined using deionised water. It is known that high-intensity carbon peaks could be encountered when machining in hydrocarbon-based dielectric liquid.

At 5 g/l SiC powder concentration and 2 A pulse current, the surface formation was altered with increasing pulse on time from 25 μ s to 100 μ s. The surface topography with a lower pulse on time (25 and 50 μ s) constitutes more craters with sharp peaks led to more even surfaces as shown in Fig. 6(a, b). However, more visible subtle surface asperities were formed at 100 μ s pulse on time as shown in Fig. 6(c), which led to the pebbling-like uneven surface.

When machining with 10 g/l SiC powder concentration, 2 A pulse current and 25 μ s pulse on time gives the most regular surface as shown in Fig. 7(a). Increasing the pulse on time at the same current level develops the surface irregularities as shown in Fig. 7(b, c). On the other hand, the surface becomes more regular when using high pulse on times and 7 A pulse current as shown in Fig. 7(d, e, f) that are in contradiction with the 2 A pulse current case.

Using low SiC concentration such as 5 g/l at 25 μ s pulse on time and 7 A pulse current leads surfaces with smooth and regularly distributed craters compared to higher concentration cases such as 20 g/l as shown in Fig. 8.

Backscattered SEM images also reveal differences in surface composition. The main noticeable distinctness is the contrast between the base material and the SiC particles. A dark and powder-parent metal complex structured areas are observed on the surface as shown in Fig. 9(a) when using 5 g/l powder concentrations, 50 μ s pulse on time and 2 A pulse current. Increased powder concentration revealed accumulated regions as shown in Fig. 9(b) and a further increase in concentration to 20 g/l led the SiC particles to spread on the surface and result in relatively homogeneous distribution as shown in Fig. 9(c). On the other hand, there is no visible dark and complex areas and likewise hardly seen SiC particles when machining using 7 A pulse current and both of 5 and 10 g/l SiC concentration cases as shown in Figs. 9(d) and (e), respectively. However, SiC particles again spread on the surface with a relatively low number of occasions as shown in Fig. 9(f) with the use of 20 g/l SiC mixed dielectric liquid.

The XRD profiles of surfaces machined in deionised water, and SiC added powder cases (Fig. 10) indicate the most of the peaks match with α Ti, β Ti and TiO. However, peaks, corresponding to TiC and possible Si including complex phases, observed for the sample machined in SiC powder mixed dielectric liquid that confirms the material migration phenomena during machining.

The surface roughness is increasing with an increase in pulse current as expected. The general trend also conveyed when using 10 and 20 g/l SiC powder concentration in the dielectric liquid as shown Fig. 11. However, the general trend is disturbed with the use of 2A pulse current and 5 g/l SiC powder mixing in the dielectric liquid as shown in Fig.11(a). The average surface roughness is 6.77 μ m for 25 μ s pulse on time which is relatively higher than the surface roughness measured for 50 μ s pulse on time. The result is not a surprise since the surface irregularities considerably increased due to uneven distribution of secondary discharges during machining.

3.2 SiC particles deposition to the surface

The number of particles deposited on the surface was counted from an actual SEM image which was 0.1133 mm². Only sharp-edged particles accepted as SiC particles migrated from

the dielectric to the surface. Then, predicted numbers of the particle expanded to the unit area in mm^2 . Relatively, a high number of particles deposited on the surface when using 5 g/l concentration and 2 A pulse current as shown in Fig. 12(a). However, increasing the SiC concentration in dielectric liquid to 10 g/l and using the same current level suppressed the number of deposited particles for 50 and 100 μs pulse on times as shown in Fig. 12(b). From among all concentrations, 20g/l represented the most efficient cases regarding SiC particle migration to the machined surface. Interestingly, the highest amount of SiC particle deposition is observed when using 50 μs pulse on time for both pulse currents. The powder transfer mechanism works for 25 μs pulse on time, increases abruptly and formed a peak when the pulse on time increased to 50 μs for both of the pulse current levels as shown in Fig. 12(c). Lastly, a further increase in pulse time to 100 μs result in a decrease in the powder deposition especially for samples machined using 7 A pulse current.

The occurrence of secondary discharges is the main reason for improved SiC transfer in particulate form. Increasing the pulse current deplete the material transfer mechanism in particulate form due to the insufficiency of secondary discharges. Therefore, the formation of the dark layer is suppressed for all samples machined using 7A pulse current. Microhardness measurements rely on the hardness of distinctive layers, and the dark layer is the hardest one among them. Consequently, it is right to assume relatively softer structures due to the absence of the dark layer when machining in 7 A pulse current setting.

Moreover, Analysis of Variance (ANOVA) is carried out for the number of particles deposited on the surfaces to identify the significance of each factor (Table 4). Percentage contribution of each factor to particles deposited on the surface is determined by dividing adjusted sum of squares (Adj SS) to total adjusted sum of squares (Total Adj SS) values. According to ANOVA result, the particles concentration is the most influential factors (%36.02) followed by pulse current (%26.33) for the deposition of SiC particles on the surface.

3.3 Sectional analysis and microhardness

Subsurface layers with PMEDM with different concentration also show impressive results. Subsurface layers are composed of a combination of various layers which include an uppermost dark layer when the samples were machined with specific machining conditions. A featureless white layer following some dendritic-like structures beneath it could be considered as the portion of the material that the transformations took place in the liquid phase during

machining. A tempered layer, and finally the base material lay beneath the layers. The formation of a dark structure layer over the white layer was observed when using 2A pulse current, low SiC concentration in dielectric and high pulse on time as shown in Fig. 13. The overall thickness of affected layers decreases with an increase in powder concentration. Comparing the predicted SiC particle numbers together with section views reveals that machining with 2 A pulse current and 50 μ s pulse on time gives the highest number of embedded particles to the surface. Meantime, the surface is smoother and have one of the thinnest heat affected layers (white layer and tempered layer) where the formation of dark and dendritic structures was suppressed. On the other hand, the lowest number of embedded particles was observed when using 100 μ s pulse on time in 10 g/l SiC concentration dielectric liquid where the continuous dark-structured layer formed over the white layer. However, the formation of the dark layer is suppressed for all samples machined using 7A pulse current, and similar heat affected layers was observed as in Fig. 14.

The microhardness of various types of heat affected layers is also of interest to explain the interactions with the suspended powders in the dielectric liquid. The electrical parameters were selected as 100 μ s pulse on time and 2 A pulse current since the all variety of heat affected layers were encountered under the machining conditions. Moreover, one additional sample was machined without using powder additive in deionised water to compromise the results with the SiC powder additive cases. Among the heat affected layers, the uppermost dark layer was tagged as “d” on the section view. In some cases, dendritic features that represent the confrontation of phase change isotherms formed beneath the layer and tagged as “c”. A fine structure of α phase rich region is beneath the layer where the transformations occurred in the liquid phase (“b”). After this thin layer, a tempered zone (“a”) and lastly the base structure of the work material are followed.

Machining in water without powder additives suppressed the formation of dendritic structures beneath the dark layer as shown in Fig. 15(a). The microhardness of tempered and white layers is comparable to the base material and suddenly increased in the dark layer where the average is 1701 HV. Adding 5 g/l SiC powders in dielectric liquid favored the formation of dendritic-like features beneath the dark layer and indicated a considerable increase in microhardness with an average of 1401 HV as shown in Fig. 15(b). The average hardness of the dark layer also gradually rose to 1896 HV. The thickness of overall heat affected layers decreased with an increase in SiC powder concentration to 10 g/l where the average microhardness values of dendritic-like features and dark layer increased which are 1500 and

1928 HV, respectively, as shown in Fig.15(c). Further, decrease in overall affected layer thickness and increase in average microhardness values are essential when machining with 20 g/l SiC powder additives in dielectric liquid as shown in Fig. 15(d). The highest value of average microhardness in the dark and dendritic layer are gathered in the case that is 2217 HV and 1772 HV, respectively.

3.4. Discussion of the results

Suspended particles in dielectric liquid alter the breakdown conditions during sparking and both extensively affect the features of machined surfaces and subsurface microstructures in EDM. Generation of several breakdown regions at the initial stages of discharging decrease the breakdown strength of the dielectric liquid and result in appropriate conditions for discharging with enlarged inter-electrode gap [20]. Increased inter-electrode gap distance not only improves cleaning cycles between successive discharges with the use of circulation system but also increase the number of suspended particles in the gap. Then, the movement of particles under the electrical field became a significant concern during discharging. Previous studies indicate that different types of suspended particle motion are possible such as reciprocating, adhesion to electrodes, cluster stagnation or chain stagnation within the gap [21]. In each case, the discharge channel confronts with the suspended particles which lead separation of the primary discharge channel during machining. Therefore, it could be concluded that the changes on the machined surface are directly associated powder concentration in the dielectric liquid as well as the electrical parameters such as pulse on time and current. In the previous study [19] several discharge channel separation forms were suggested in the view of surface textural changes and subsurface heat affected layers for a wide variety of electrical parameters but constant powder concentration in PMEDM. The thickness of the re-solidified layer increases with the generation of single or unevenly distributed discharges during machining. Since the energy intensities of discharges are high enough to melt deeper portions of material. SiC particles confronted with electrical discharges during machining decompose partly or wholly within the plasma channel. Such decomposition alters the composition of the re-solidified layer in terms Aluminium silicates. The XRD patterns confirm the formation of such complicated phases within the layer. The expected impact of such compositional changes also observed regarding hardness variations in the re-solidified layer. On the other hand, particles penetrated to the surface are the particles placed close to a discharge column and directed towards the melted metal pool due to the sudden closure of the plasma channel that generates high negative pressures at the end

of discharge period. Therefore, it could be concluded that two different migration mechanism takes places during machining. The migration in particulate form amplified when the main discharge channel subdivided into several secondary discharges. In this way, the suspended particles in dielectric liquid stuck among the scattered sub discharges that increased the probability of penetrating into the melted metal pool at the end of the pulse

The microhardness measurements of the heat affected layers reveal the interactions with the suspended particles. If machining is conducted without SiC powder addition in a dielectric liquid, the re-solidified layer hardness is relatively lower than that of the additive cases. The main discharge channels confront with some suspended particles and partially or completely decompose it. Then, the channel becomes rich of decomposed suspended materials ions that alloy the re-solidified layer and explains the increase in its hardness with the increase in SiC powder concentration in the dielectric liquid. However, the overall thickness of the heat affected layer decreases as in increase in powder concentration. This result is not a surprise since increased number of confrontations with the powder particles during machining divides the main discharge channel into more number of sub-discharges that means divided heat sources on an enlarged area during discharging. Therefore, increase in powder concentration in dielectric liquid result in the progressive division of primary discharges into evenly distributed sub-discharges. Such further division also leads a unique state where the suspended particles surrounded with sub-discharges. Finally, the particles move toward the molten cavities with the cease of a discharge and penetrate to the surface.

The number of particles transferred to the machined surface reveals the dependency of the pulse current. Low pulse currents and high suspended particle concentration in dielectric liquid enhance the particle transfer mechanism. This result could be attributed to the easiness of discharge division with the use of low current levels during machining. The electrical field is weaker and therefore more sensitive to the non-continuities created by the suspended particles.

4. Conclusions

Altered discharge conditions during sparking due to the suspended particles in dielectric liquid extensively affect the features of machined surfaces and subsurface microstructures in PMEDM. The changes are directly associated with the operational parameters such as pulse current, pulse on time and powder concentration in the dielectric liquid. Plasma channel

interacts with the suspended SiC particles and initiates different mechanisms during machining. In the view of this study and parameters, the following conclusions can be drawn:

- It was observed that low pulse currents and high suspended particle concentration in dielectric liquid enhance the material transfer mechanism in particulate form.
- According to the ANOVA, the most influential factors for particle transfer is the particle concentration followed by the pulse current and pulse on time.
- The re-solidified layer thicknesses decrease with an increase in SiC powder concentration in the dielectric liquid. However, the layer hardness increases due to material transferred from the dielectric liquid.
- The particle transfer mechanism also differs regarding suspended particle concentration in the dielectric liquid. The powder particles during machining disturb the main discharge channel form and divide it into sub-discharges. Therefore, increase in powder concentration in dielectric liquid result in the following division of primary discharges into evenly distributed sub-discharges.
- The formation of secondary discharges favoured the improved SiC transfer in particulate form. However, increasing the pulse current deplete the material transfer mechanism in particulate form due to the inadequacy of secondary discharges.

Acknowledgements

The authors extend sincere thanks to The Bülent Ecevit University Research Program and Liverpool John Moores University for the grants given on the subject, which otherwise the work would not be initiated.

References

1. Zaman HA, Safian S, Idris MH, Kamarudin A. Metallic biomaterial for medical implant applications: a review. *Applied Mechanics and Materials* 2015; 735: 19–25.
2. Li Y, Yang C, Zhao H, Qu S, Li X, Li Y. New developments of Ti-based alloys for biomedical applications. *Materials* 2014;7 (3): 1709–1800.
3. Erden A, Bilgin S. Role of Impurities In Electric Discharge Machining; In *Proceedings of the 21st International Machine Tool Design and Research Conference, Swansea, UK, Sept 8-12, 1980*, J.M. Alexander, Eds.; Macmillan Education: UK, 1980.

4. Jeswani ML. Effects of the addition of graphite powder to kerosene used as the dielectric fluid in electrical discharge machining. *Wear* 1981; 70(2): 133–9.
5. Singh B, Kumar J, Kumar S. Investigation of the Tool Wear Rate in Tungsten Powder-Mixed Electric Discharge Machining of AA6061/10%SiCp Composite. *Mater Manuf Process* 2016; 31(4): 456-66.
6. Kumar J, Kumar S. Influences of Process Parameters on MRR Improvement in Simple and Powder-Mixed EDM of AA6061/10%SiC Composite. *Mater Manuf Process* 2015; 30(3): 303-12.
7. Kuriachen B, Mathew J. Effect of Powder Mixed Dielectric on Material Removal and Surface Modification in Microelectric Discharge Machining of Ti-6Al-4V. *Mater Manuf Process* 2016; 31(4): 439-46.
8. Zhao WS, Meng QG, Wang ZL. The application of research on powder mixed EDM in rough machining. *J Mater Process Technol* 2002; 129(1-3): 30–3.
9. Pecas P, Henriques EA. Influence of silicon powder mixed dielectric on conventional electrical discharge machining. *Int J Mach Tool Manu* 2003; 43(14): 1465–71.
10. Rehbein W, Schulze HP, Mecke K, Wollenberg G, Storr M. Influence of selected groups of additives on breakdown in EDM sinking. *J Mater Process Technol* 2004; 149(1-3): 58–64.
11. Ekmekci B, Ersoz Y. How suspended particles affect surface morphology in powder mixed electrical discharge machining (PMEDM). *Metall Mater Trans B* 2012; 43(5): 1138–48.
12. Amorim FL, Dalcin VA, Soares P, Mendes LA. Surface modification of tool steel by electrical discharge machining with molybdenum powder mixed in dielectric fluid. *Int J Adv Manuf Tech* 2016; 91(1-4):341-50.
13. Ekmekci N, Ekmekci B. Electrical Discharge Machining of Ti6Al4V in Hydroxyapatite Powder Mixed Dielectric Liquid. *Mater Manuf Process* 2016; 31(13): 1663-70.
14. Li L, Feng L, Bai X, Li ZY. Surface characteristics of Ti-6Al-4V alloy by EDM with Cu-SiC composite electrode. *Appl Surf Sci* 2016; 388: 546–50.
15. Shabgard M, Khosrozadeh B. Investigation of carbon nanotube added dielectric on the surface characteristics and machining performance of Ti–6Al–4V alloy in EDM process. *J Manuf Process* 2017; 25: 212–9.
16. Li L, Zhao L, Li ZY, Feng L, Bai X. Surface characteristics of Ti-6Al-4V by SiC abrasive-mixed EDM with magnetic stirring. *Mater Manuf Process* 2017; 32(1): 83-6.

17. Prakash C, Kansal HK, Pabla BS, Puri S. Experimental investigations in powder mixed electric discharge machining of Ti-35Nb-7Ta-5Zr β -titanium alloy. *Mater Manuf Process* 2017; 32(3): 274-85.
18. Yaşar H, Ekmekci B. A Comparative Study on Powder Mixed Electrical Discharge Machining of Ti-6Al-4V; In 18th International Conference on Advances in Materials and Processing Technologies, Madrid, Spain, Dec 14-17, 2015.
19. Ekmekci B, Yaşar H, Ekmekci N. A Discharge Separation Model for Powder Mixed Electrical Discharge Machining. *J Manuf Sci E-T Asme* 2016;138(8): 081006-1-9.
20. Chow H-M, Yan B-H, Huang F-Y, Hung J-C. Study of Added Powder in Kerosene for the Micro-Slit Machining of Titanium Alloy Using Electro-Discharge Machining. *J Mater Process Technol* 2000; 101(1-3): 95-103.
21. Furutani K, Saneto A, Takezawa H, Mohri, N, Miyake H. Accretion of Titanium Carbide by Electrical Discharge Machining with Powder Suspended in Working Fluid. *Precis Eng* 2001; 25(2): 138-44.

Figures Captions

Figure 1. (a) EDM setup schematic view, (b) EDM setup reservoir view, (c) EDMed sample, (d) Heat affected layers' measurement.

Figure 2. An example of SEM image showing SiC particles deposited onto the EDMed surface.

Figure 3. An image of indentation during microhardness measurement from the section

Figure 4. SEM images of PMEDMed samples (a) Concentration= 5 g/l, (b) Concentration= 10 g/l, (c) Concentration= 20 g/l (Pulse current: 2 A, Pulse on time: 100 μ s, magnification: X200).

Figure 5. (a) SEM view and (b) EDS analysis of PMEDM'ed Ti-6Al-4V surface (c) EDS analysis of selected particle. Pulse current: 2 A, pulse on time: 100 μ s and concentration: 20g/l, magnification: X1000.

Figure 6. The 3D surface topography of samples. Concentration: 5 g/l, pulse current: 2A magnification: X50.

Figure 7. The 3D topography of samples. Powder concentration: 10 g/l, magnification: X10

Figure 8. The 3D surface topography of samples. Pulse on time: 25 μ s, pulse current: 7 A. magnifications: X10.

Figure 9. Back scattered SEM images of the samples. Pulse on time: 50 μ s, magnification: X1000.

Figure 10. Comparison of XRD profiles of surfaces machined in deionized water and SiC powder additive water dielectric liquid.

Figure 11. Surface roughness variation with PMEMD parameters

Figure 12. Number of SiC particles deposited on the surface

Figure 13. Section views of the specimens. Pulse current: 2 A, magnification: X250.

Figure 14. Section view of the specimen. Pulse current: 7 A, pulse on time=100 μ s, concentration= 5 g/l.

Figure 15. Heat affected layers (top picture) and microhardness characteriscs on diffeent layers (bottom picture). Pulse current = 2 A and pulse on time= 100 μ s. (a) without SiC

powder additive, (b) with 5 g/l SiC powder additive, (c) with 10 g/l SiC powder additive, (d) with 20 g/l SiC powder additive.

Tables Captions

Table 1. Chemical composition (weight %) of Ti-6Al-4V ELI used for specimens

Table 2. Factors and Levels

Table 3. Experimental parameters and results

Table 4. ANOVA results for the number of SiC particles deposited to the surface

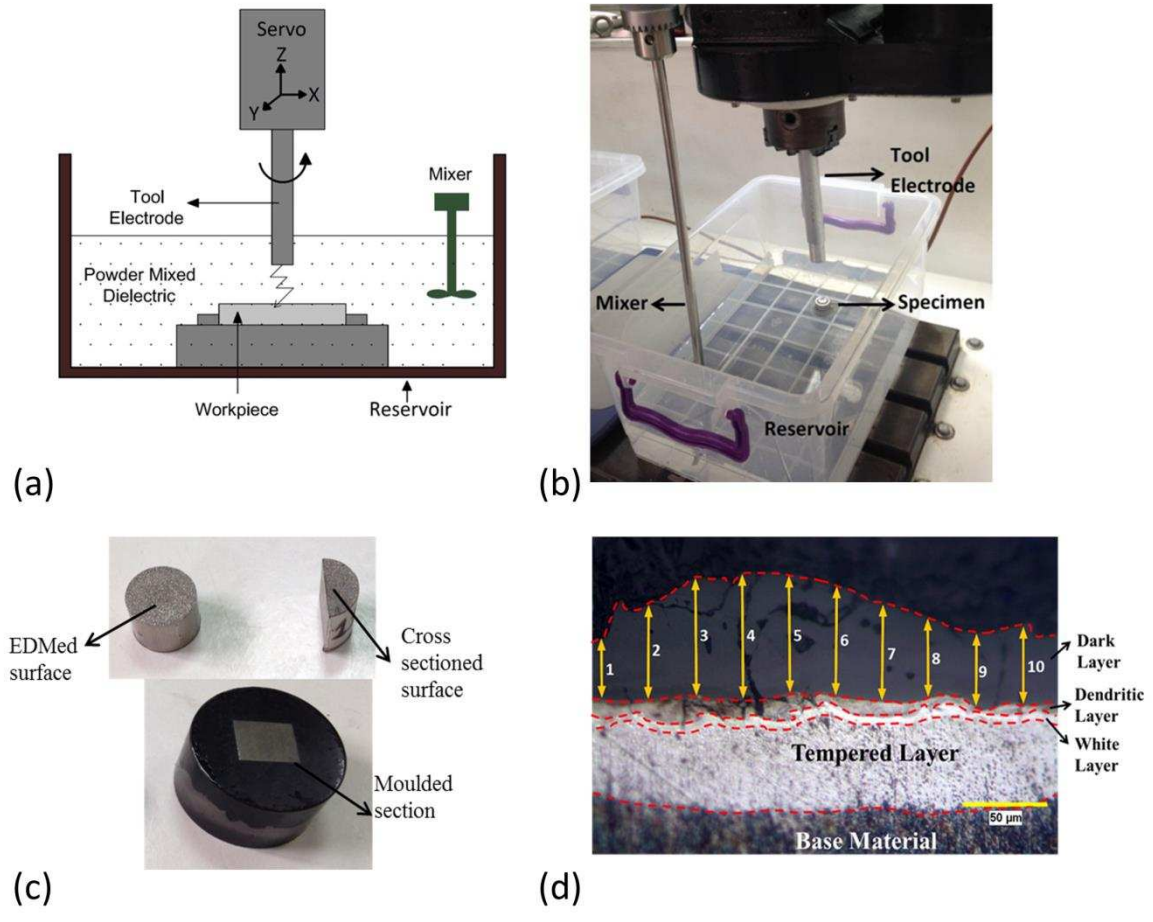


Figure 1

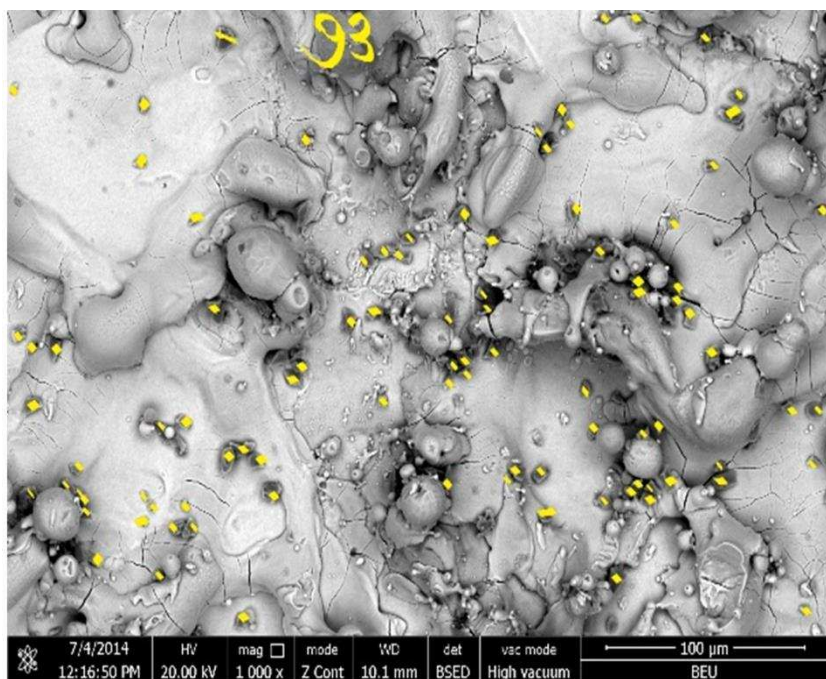


Figure 2

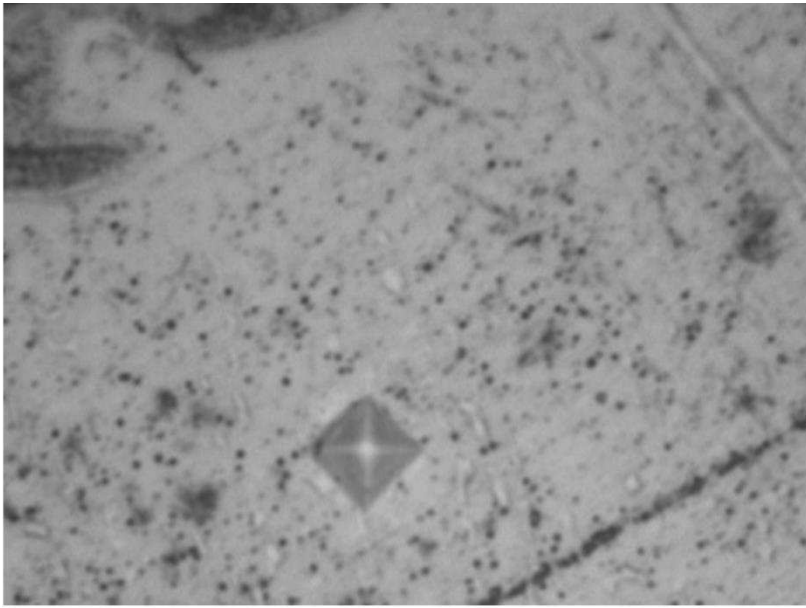
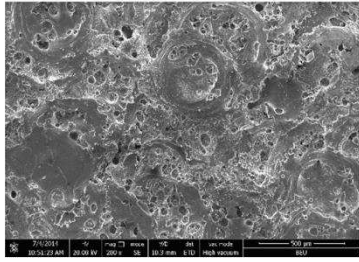
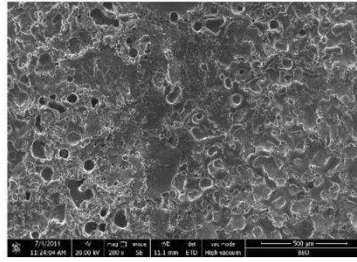


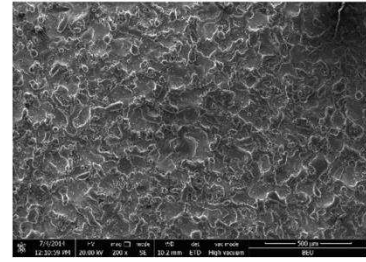
Figure 3



(a)

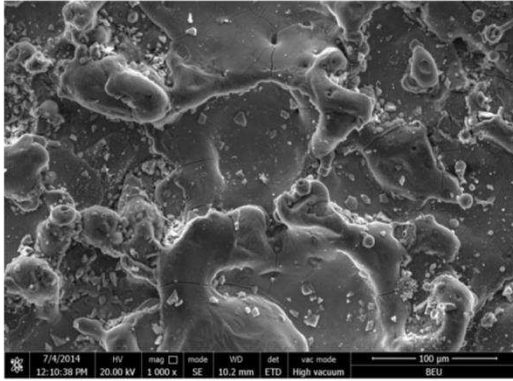


(b)

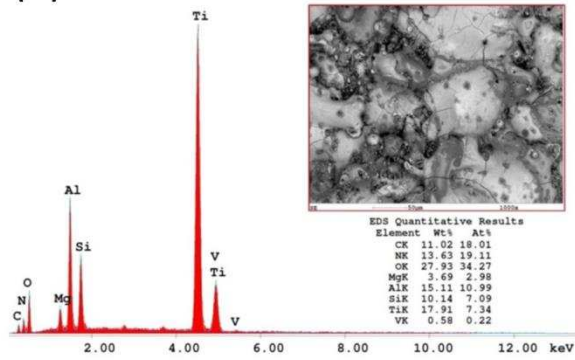


(c)

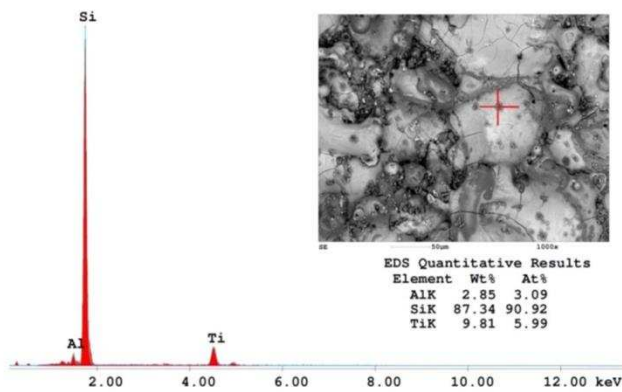
Figure 4



(a)



(b)



(c)

Figure 5

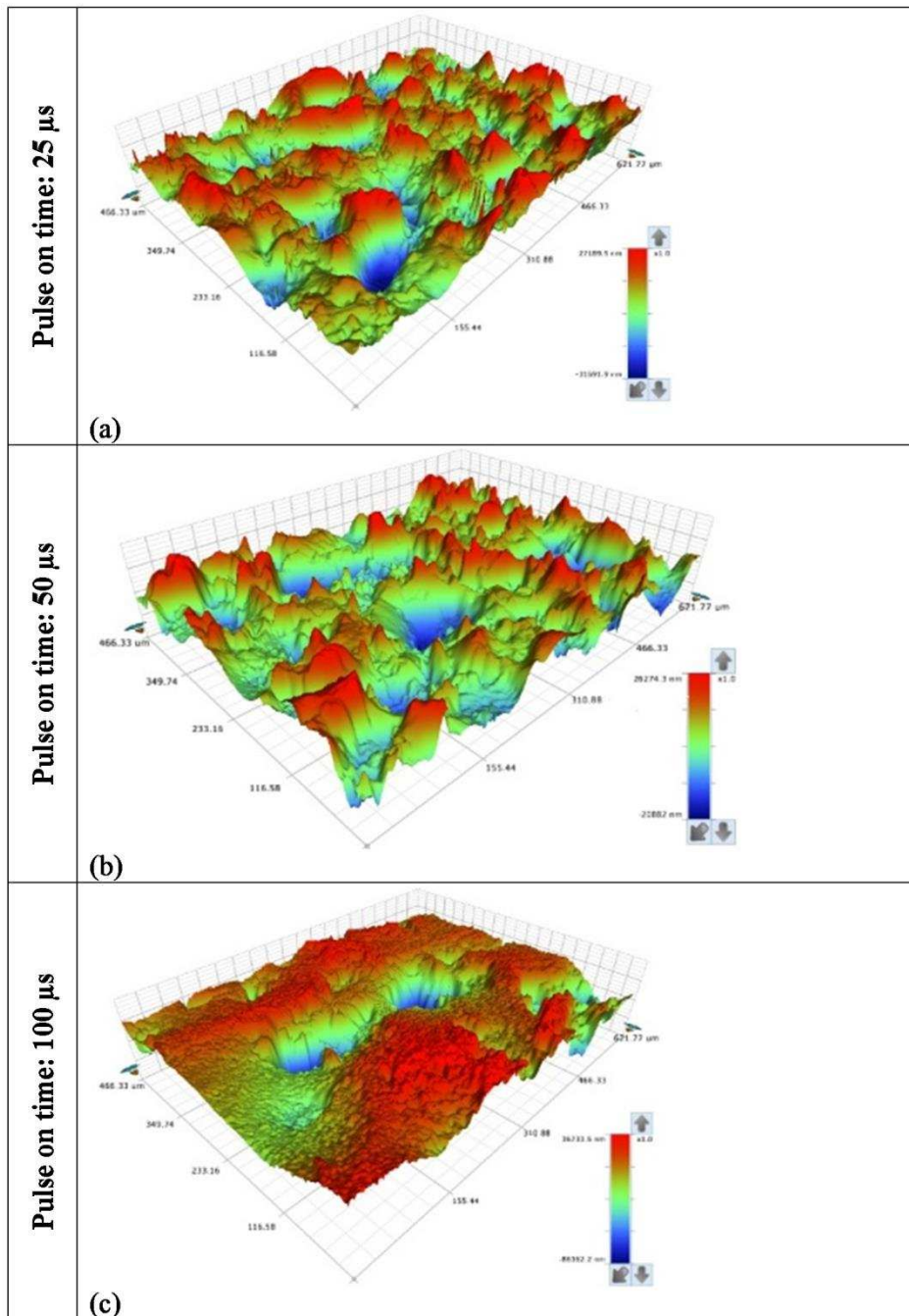


Figure 6

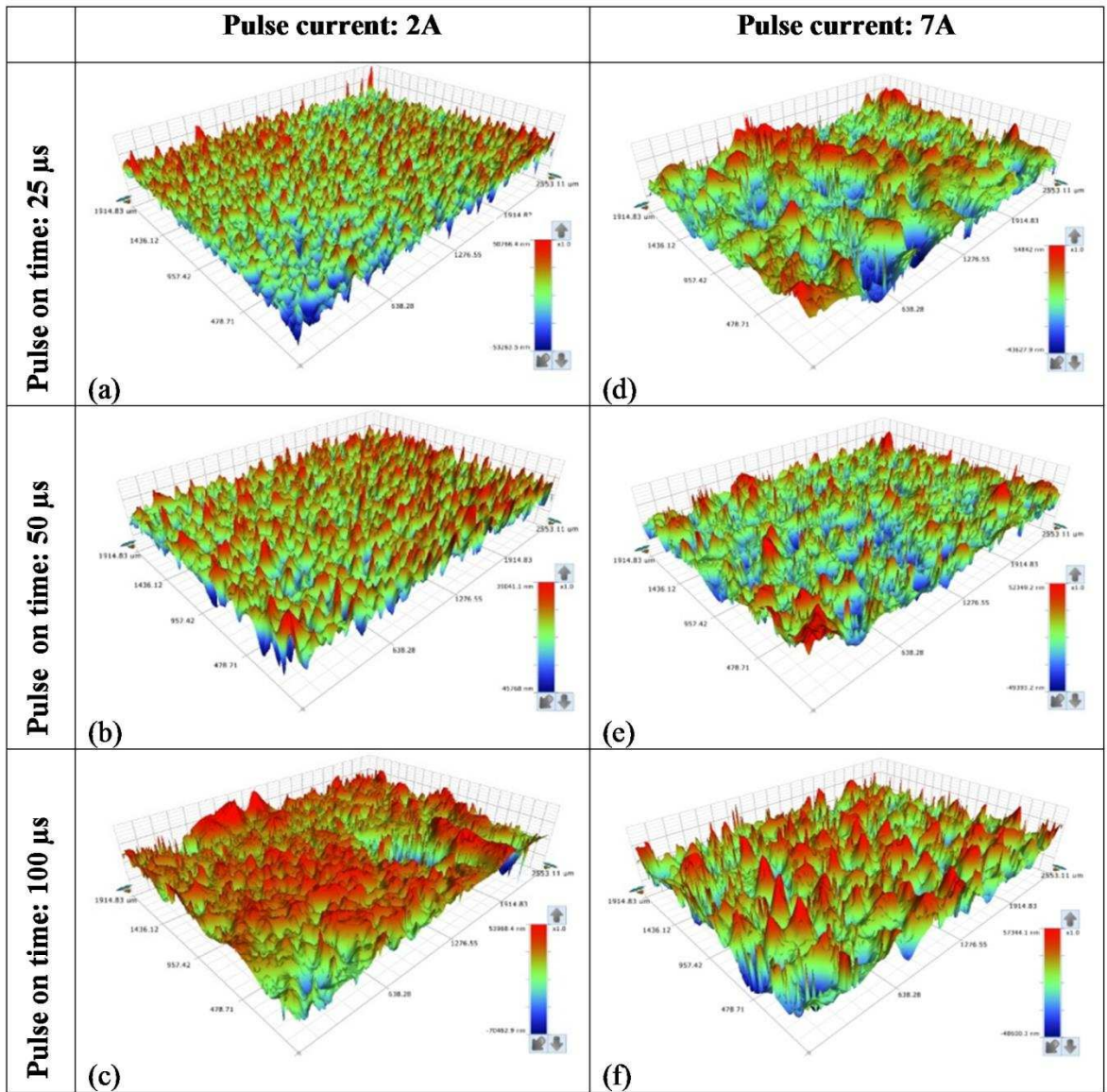


Figure 7

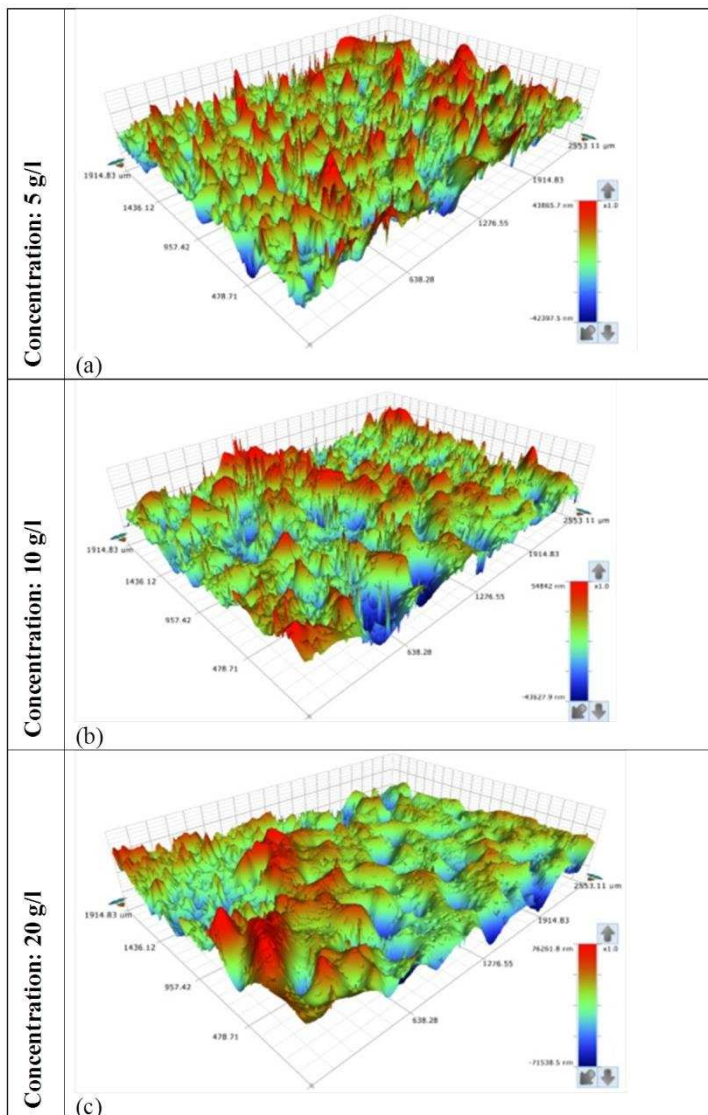


Figure 8

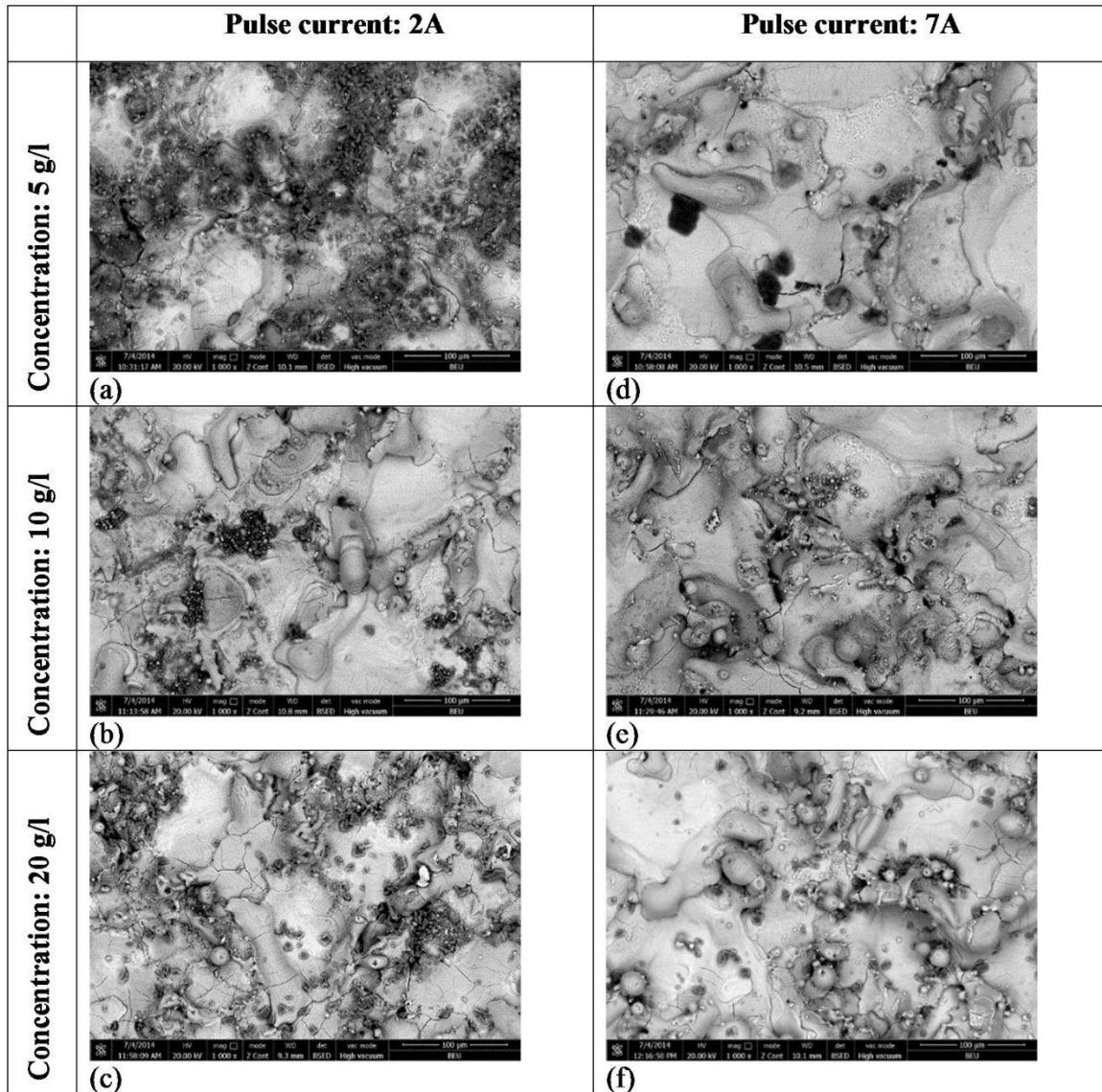


Figure 9

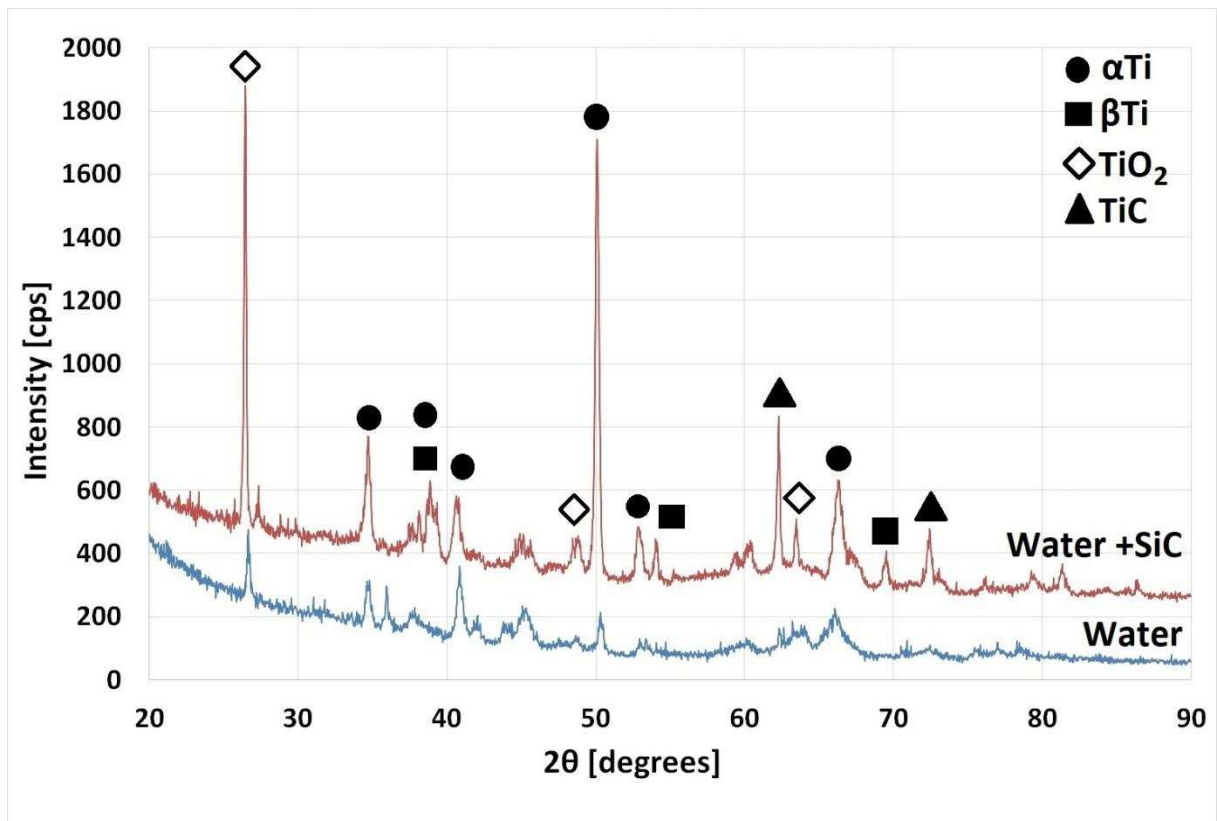


Figure 10

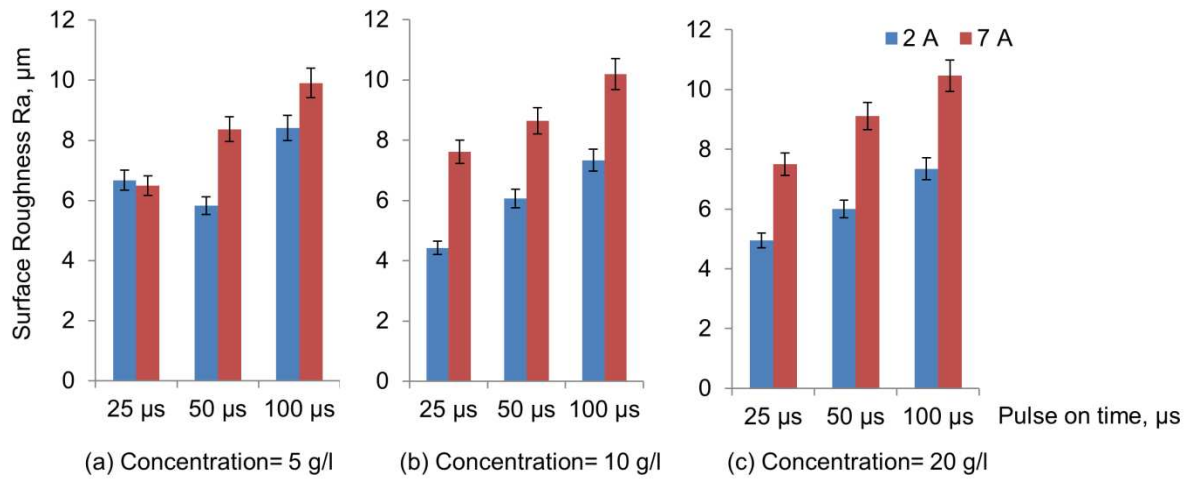


Figure 11

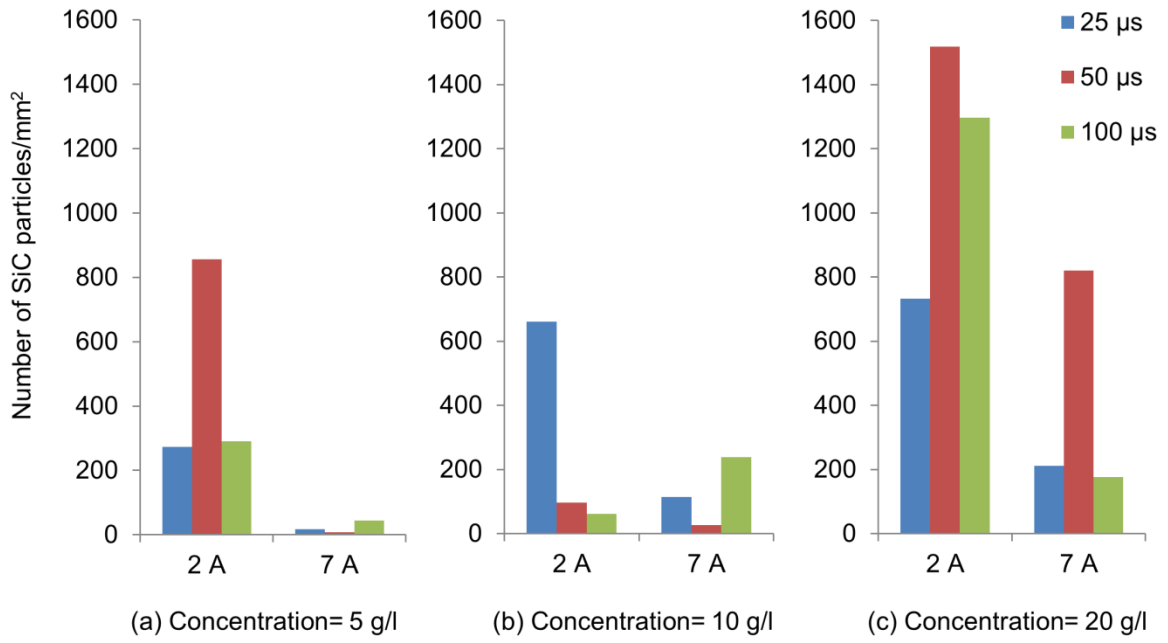


Figure 12

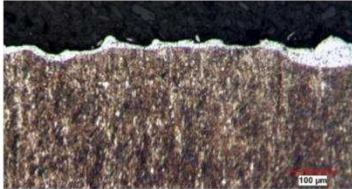
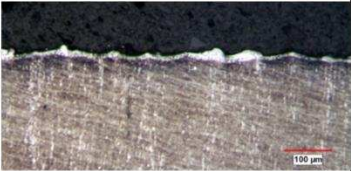

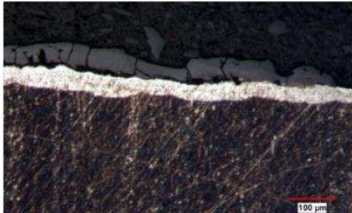
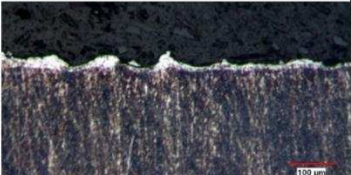
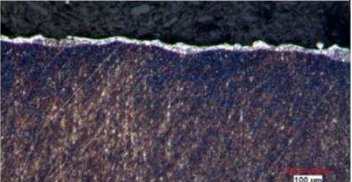



	Concentration: 5 g/l	Concentration: 10 g/l	Concentration: 20 g/l
Pulse on time: 25 μ s	 <p>(a) Predicted SiC per mm²: 273</p>	 <p>(b) Predicted SiC per mm²: 661</p>	 <p>(c) Predicted SiC per mm²: 732</p>
Pulse on time: 50 μ s	 <p>(d) Predicted SiC per mm²: 856</p>	 <p>(e) Predicted SiC per mm²: 97</p>	 <p>(f) Predicted SiC per mm²: 1518</p>
Pulse on time: 100 μ s	 <p>(g) Predicted SiC per mm²: 291</p>	 <p>(h) Predicted SiC per mm²: 61</p>	 <p>(l) Predicted SiC per mm²: 1297</p>

Figure 13

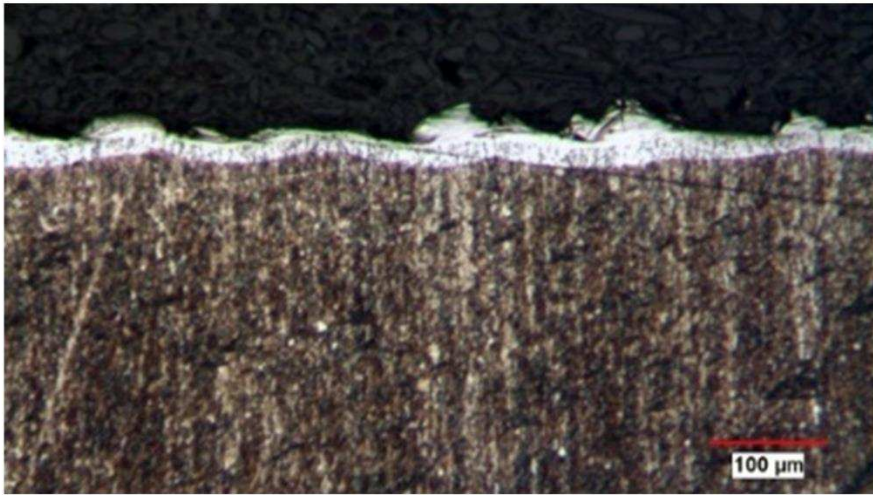


Figure 14

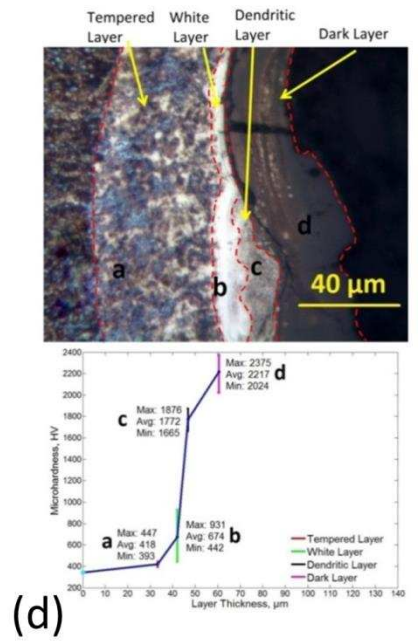
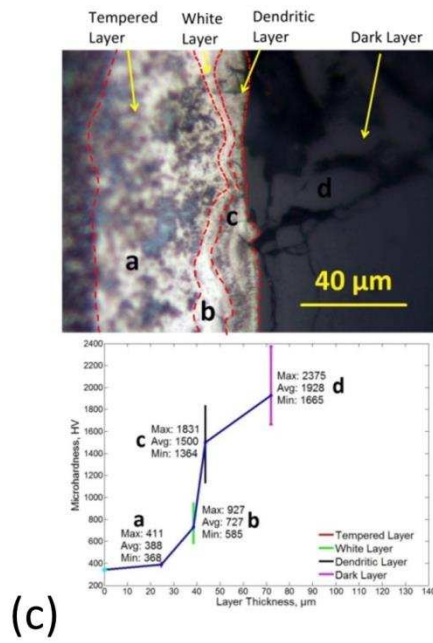
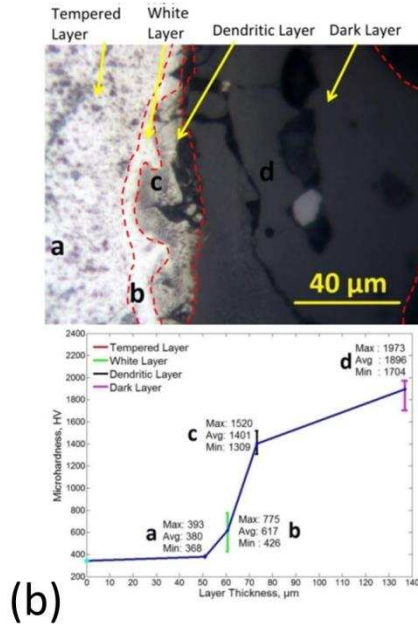
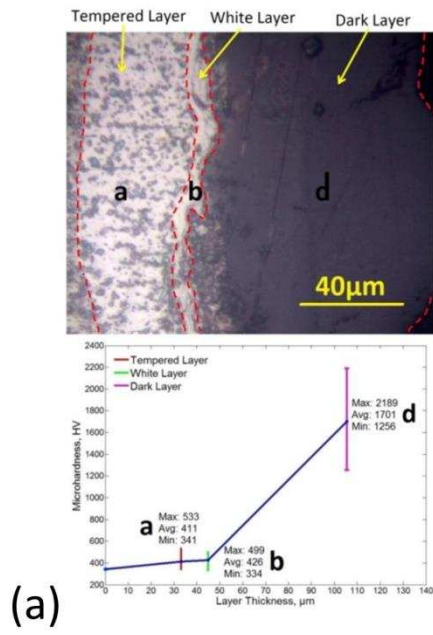


Figure 15

Table 4. Chemical composition (weight %) of Ti-6Al-4V ELI used for specimens

Ti	Al	V	Fe	O	C	N	H
89.551	6.15	4.06	0.10	0.09	0.02	0.028	0.001

Table 5. Factors and Levels

Factors	Level 1	Level 2	Level 3
Pulse Current (A)	2	7	-
Pulse on Time (μ s)	25	50	100
Concentration (g/l)	5	10	20

Table 6. Experimental parameters and results

Exp. No	Input parameters			Results		
	Pulse Current (A)	Pulse on Time (μ s)	Concentration (g/l)	Surface Roughness Ra (μ m)	Number of SiC particles in actual SEM area (0,1133 mm ²)	Predicted number of SiC particles per mm ² (adapted from the actual SEM area)
1	2	25	5	6.77	31	273
2	2	25	10	4.48	75	661
3	2	25	20	5.03	83	732
4	2	50	5	5.01	97	856
5	2	50	10	5.88	11	97
6	2	50	20	6.76	172	1518
7	2	100	5	8.55	33	291
8	2	100	10	6.67	7	61
9	2	100	20	7.93	147	1297
10	7	25	5	5.60	2	17
11	7	25	10	5.94	13	114
12	7	25	20	6.32	24	211
13	7	50	5	8.16	1	8
14	7	50	10	8.52	3	26
15	7	50	20	8.56	93	820
16	7	100	5	9.89	5	44
17	7	100	10	9.20	27	238
18	7	100	20	8.75	20	176

Table 4. ANOVA results for the number of SiC particles deposited to the surface

Analysis of Variance						
Source	DF	Adj SS	Adj MS	F-Value	P-Value	Percentage contribution (%)
Pulse Current (A)	1	952200	952200	9.65	0.009	26.33
Pulse on Time (μ s)	2	177077	88538	0.90	0.433	4.90
Concentration (g/l)	2	1302524	651262	6.60	0.012	36.02
Error	12	1184401	98700			32.75
Total	17	3616202				